Distributed Atomic Polarizabilities of Amino Acids and their Hydrogen-Bonded Aggregates

Leonardo H. R. Dos Santos,*,† *Anna Krawczuk*,‡ *and Piero Macchi*,*,†

† Department of Chemistry and Biochemistry, University of Bern, Freiestrasse 3, 3012 Bern, Switzerland

‡ Faculty of Chemistry, Jagiellonian University, Ingardena 3, 30-060 Kraków, Poland

ABSTRACT

With the purpose of rational design of optical materials, distributed atomic polarizabilities of amino acid molecules and their hydrogen-bonded aggregates are calculated in order to identify the most efficient functional groups, able to buildup larger electric susceptibilities in crystals. Moreover, we carefully analyze how the atomic polarizabilities depend on the one-electron basis set or the many-electron Hamiltonian, including both wave function and density functional theory methods. This is useful for selecting the level of theory that best combines high accuracy and low computational costs, very important in particular when using the *cluster* method to estimate susceptibilities of molecular-based materials.

KEYWORDS: distributed polarizability, quantum theory of atoms in molecules, electron density distribution, linear optical properties, hydrogen bonding.

1. INTRODUCTION

The response of a molecule to an electric field has received enormous attention from computational chemists, due to the important implications for opto-electronic properties of materials.[1-3] The linear and non-linear optical responses are correlated to the dipole electric (hyper)polarizabilities and susceptibilities at molecular and macroscopic levels, respectively.[4] With the current computational resources, (hyper)polarizabilities of medium-size molecules in the gas-phase can be computed with satisfactory accuracy if sufficient electronic correlation is included and extended atomic basis sets are used. This has enabled the design of molecular-based optical materials, but, as stated by Champagne and Bishop,[5] the knowledge acquired in the field of single-molecule (hyper)polarizability calculations must evolve to quantitatively rationalize optical properties of the solid state, a field which is far less advanced. In fact, with few exceptions, a useful electro-optical material will be in the solid state and, frequently, in a crystalline or partially crystalline phase. For this reason, the ultimate goal is the investigation of optical properties in periodically homogeneous systems.

Crystal-orbital or plane-wave-based calculations are in principle the correct approaches to model crystalline effects. However, some problems affect these methods: a) the amount of electronic correlation that one can introduce is limited;[6] b) convergence often fails when crystal-orbital Bloch-type wave functions contain diffuse atomic functions; c) plane-wave calculations exclude the localized core-orbital functions and therefore their contribution to the (hyper)polarizabilities. In order to overcome these drawbacks, some approaches have emerged, for example the so-called supermolecule or cluster method.[5] Within this approach, the (hyper)polarizabilities of several interacting molecules are evaluated as a whole, just like in standard molecular

calculations. The (hyper)polarizabilities of a molecule embedded in a crystal are then estimated as average quantities over the cluster, and eventually used to approximate the electric susceptibilities of a periodic system. By comparing the (hyper)polarizabilities of an isolated molecule and that extracted from the molecular cluster, one gains insight into the role of short and medium-range intermolecular interactions, crucial for the design of optical materials.[7]

Because density functional theory (DFT) methods may be inappropriate for correct evaluation of the intermolecular dispersion forces, one of the goals of the present work is to identify the most accurate DFT functionals able to estimate optical properties in molecular assemblies, using calculations of high-level electron correlation as benchmarks. The performance of DFT have been rigorously investigated for the polarizabilities of large water clusters.[8] It was found that the accuracy of post-Hartree-Fock levels of theory was not sufficiently higher than that of DFT to justify the increased computational costs. In this work, we aim at extend this analysis to amino acid aggregates, through a careful estimation of the cost/benefits and the *marginal utility* of extending the level of theory.

A subject that has also attracted attention is the breakdown of the molecular polarizability into atomic contributions.[9] Visualizing and analyzing atomic and bond polarizabilities of a system is useful because functional groups represent the way in which chemists reduce molecules for synthetic and engineering purposes. In fact, a given molecular property may especially originate from one particular group. In this respect, the transferability of atomic and functional group properties is a key concept which allows exporting quantities, calculated with high accuracy in

small reference molecules, to atoms or functional groups belonging to complex systems, like macromolecules, polymers or crystals,[10-12] that would be too expensive to calculate *ab initio*.

Several schemes have been proposed for the calculation of distributed atomic polarizabilities.[13-21] Bader and co-workers[22] adopted the topological partitioning of the electron density within the Quantum Theory of Atoms in Molecules (QTAIM). The method has been successfully applied for the evaluation of intermolecular interaction energies[23-25] and the transferability of electrostatic properties in *n*-alkanes.[26] Subsequently, Keith[27] generalized Bader's method, within the "atomic response theory", recently modified and implemented in a program (*PolaBer*) by some of us.[28] The main advantage is the removal of origin-dependent terms, which are particularly disadvantageous for the transferability of atomic or group quantities. *PolaBer* extends the quantities computed from the atomic polarizabilities, including bond polarizabilities and evaluation of refractive indices in crystals.

In fact, QTAIM offers several advantages, in particular because it leads to an exact partitioning of the molecular electron density in real-space, in contrast with the Hilbert-space schemes such as the one developed by Stone[29,30] in the framework of the distributed multipole analysis.[31] Recently, the fuzzy Hirshfeld partitioning scheme of the electron density has also been applied to extract molecular polarizabilities in clusters[32,33] or atomic polarizabilities in large molecular systems.[9] However, a disadvantage of the Hirshfeld scheme, at least in the current implementations, is that the functional-group polarizabilities remain origin-dependent and, therefore, cannot be properly exported to other systems.

In the present work, the QTAIM distributed atomic first-order dipole polarizabilities of amino acids and their hydrogen-bonded aggregates are calculated at different theoretical levels. We focused on the first-order polarizability tensor $\boldsymbol{\alpha}$ due to its relative simplicity, its major role in both qualitative and quantitative considerations of reaction paths and molecular interactions, and, of course, its prominence in determining linear optical properties of materials. For this analysis, we have chosen the natural α-amino acids in their zwitterionic form, because the optical properties of their crystals, co-crystals, salts and metal hybrids have attracted much attention in the last few years.[34]

While some components of the total polarizability tensors are measurable, either in the gas or in the condensed phase,[35] no procedure is available for the experimental determination of polarizabilities of atoms in molecules. Therefore, for benchmarking the various DFT functionals, we use post-Hartree-Fock methods up to coupled-cluster (CC) techniques, known to deliver highly accurate polarizabilities.[8]

Another purpose of our work is testing the efficiency of Gaussian-type basis sets for the calculations of distributed polarizabilities. Both Pople and Dunning families of basis sets are considered. These investigations allow us to propose a protocol for the evaluation of optical properties of molecular materials that is both quality- and cost-oriented.

The last goal of our study is to quantify the perturbation of hydrogen bonds on the molecular polarizabilities, analyzing the most common aggregation modes of amino acids in the solid state.

2. THEORETICAL METHODS

2.1. Electron density calculations

Electron densities were obtained by molecular-orbital wave function calculations at various levels of approximation. We used the glycine molecule and three hydrogen bonded dimers as references in order to test various basis set expansions and to compare results from different DFT functionals against those from configuration interaction (CI) or perturbation methods (second-order Møller-Plesset, MP2). Firstly, the polarizabilities of the glycine monomer and the dimers were investigated with increasing level of electron correlation, up to coupled-cluster singles-and-doubles (CCSD), and increasing basis-set rank, up to quadruple-zeta quality including diffuse and polarization functions. Secondly, the polarizability of the glycine monomer was calculated using various density functionals and then compared against results at the highest electron-correlated levels. Thirdly, results with basis sets from Pople and Dunning families were compared against each other at the CAM-B3LYP level of theory, found to be one of the best-performing functional. Finally, all the 20 amino acids and some dimers were investigated at the CAM-B3LYP/d-aug-cc-pVDZ level, which was determined to be the best compromise between accuracy and computational costs.

When available, three-dimensional coordinates were taken from measured single crystal neutron diffraction data and kept frozen. This choice is necessary because the most stable configuration of the amino acids in the gas-phase is the neutral one, whereas the zwitterionic forms are the most frequently observed species in liquid solutions and crystal-phases. Because stationary points for the zwitterionic forms are normally not found in gas-phase potential energy surfaces, we could not use optimized geometries. For those amino acids in which X-ray structures only are

available, the heavier atom positions were kept at measured values and the distances to the attached H atoms were normalized to the average neutron diffraction values, as given by the International Tables for Crystallography. Because the crystal structure of lysine is not known, the calculations were performed for its cationic form, lysinium. Correlated calculations use the frozen-core approximation. All the wave-function calculations were performed using the Gaussian 09 package[36] and the corresponding charge-density distributions were partitioned in keeping with the QTAIM using the AIMAll program.[37]

2.2. Distributed polarizability calculations

The *PolaBer* program[28] was used to calculate distributed atomic polarizabilities. The method is based on QTAIM partitioning of the ground-state and field-perturbed electron densities $\rho(\boldsymbol{r})$ of a molecular system into its atomic contributions. The algorithm was already tested[38] and proved a reliable way to breakdown the molecular $\boldsymbol{\alpha}$ tensor into atomic contributions. Because the partitioning scheme is "exact", the sum of the atomic polarizabilities must coincide, a part for minor numerical imprecision, to the molecular polarizability calculated in Gaussian 09 using the coupled-perturbed Hartree-Fock (CPHF) or Kohn-Sham (CPKS) equations.

The QTAIM-based topological analysis allows one to represent the total molecular dipole moment as a sum of atomic components $\boldsymbol{\mu}(\Omega)$, where Ω is the atomic basin-volume. Each atomic dipole moment is the sum of a polarization $\boldsymbol{\mu}_p(\Omega)$ and a charge translation $\boldsymbol{\mu}_c(\Omega)$ contribution:[10]

$$\boldsymbol{\mu}(\Omega) = \boldsymbol{\mu}_p(\Omega) + \boldsymbol{\mu}_c(\Omega) = -\int_\Omega [\boldsymbol{r} - \boldsymbol{R}_\Omega]\rho(\boldsymbol{r})d\boldsymbol{r} + [\boldsymbol{R}_\Omega - \boldsymbol{R}_0]q(\Omega) \quad (1)$$

Where $q(\Omega)$ is the net charge of the atom Ω, $\boldsymbol{R}_\Omega$ is the position vector of Ω and $\boldsymbol{R}_0$ is the arbitrary origin of the molecular coordinate system. Although the origin-dependent charge-translation contribution can be converted to an alternative, origin-independent definition,[22] only recently a computationally convenient method for such calculation has been proposed.[27] It was slightly modified and implemented by some of us in the *PolaBer* software.[28]

The static first-order dipole polarizability tensor of a molecular system, $\boldsymbol{\alpha}$, is the gradient of the electric dipole moment $\boldsymbol{\mu}$ with respect to an external, uniform, and time-independent electric field $\boldsymbol{E}$:

$$\boldsymbol{\alpha} = \boldsymbol{i}\left(\frac{\partial \boldsymbol{\mu}}{\partial E_x}\right) + \boldsymbol{j}\left(\frac{\partial \boldsymbol{\mu}}{\partial E_y}\right) + \boldsymbol{k}\left(\frac{\partial \boldsymbol{\mu}}{\partial E_z}\right) \quad (2)$$

As for the dipole moment, the molecular polarizability tensor can be decomposed into additive atomic contributions:

$$\boldsymbol{\alpha} = \sum_{\Omega=1}^{N_a} \boldsymbol{\alpha}(\Omega) = \sum_{\Omega=1}^{N_a} \left[\boldsymbol{\alpha}_p(\Omega) + \boldsymbol{\alpha}_c(\Omega)\right] \quad (3)$$

Where N_a is the total number of atoms in the molecular system. $\boldsymbol{\alpha}_p(\Omega)$ and $\boldsymbol{\alpha}_c(\Omega)$ are the polarization and charge translation atomic polarizability tensors, respectively. These terms arise from the derivation of the corresponding $\boldsymbol{\mu}_p(\Omega)$ and $\boldsymbol{\mu}_c(\Omega)$ atomic dipole moments respect to the applied electric field, according to Eqn. 2.

Nuclear relaxations can also affect the computed linear and non-linear optical properties,[39,40] however they are not considered in this work, meaning that we focus only on the high-frequency electron polarizability. In further work, we will investigate this aspect as well.

Given the linear response of the electron density with respect to a sufficiently small applied field,[27] $\boldsymbol{\alpha}(\Omega)$ can be calculated by numerical differentiation, using wave functions computed at finite electric fields. Thus, the atomic polarizability components $\alpha_{ij}(\Omega)$ are evaluated as:

$$\alpha_{ij}(\Omega) = \lim_{\boldsymbol{E}\to 0} \frac{\mu_i^{E_j}(\Omega) - \mu_i^0(\Omega)}{E_j} \quad (4)$$

Where $\mu_i^{E_j}(\Omega)$ is the dipole moment component of the atomic basin Ω along the i direction computed with an applied electric field in direction j. Eqn. 4 does not take into account the coupling between atomic volume and atomic charge. For this reason, the atomic polarizability tensors result slightly asymmetric and require tensor symmetrization.[41]

Atomic and molecular polarizability tensors can be visualized as ellipsoids in the same three-dimensional space as the molecule, assuming $1\ \text{Å}^3 \equiv 1\ \text{Å}$. In this work, a scaling factor of $0.4\ \text{Å}^{-2}$ is applied to reduce the size of polarizability ellipsoids for visualization purposes.

All the amino acids under study and their aggregates have C_1 symmetry. Therefore, the first-order polarizability tensors have six different non-zero components. We report the components of the diagonalized tensors (α_{11}, α_{22}, α_{33}). The isotropic polarizability was estimated as:

$$\alpha_{ISO} = \frac{1}{3}(\alpha_{11} + \alpha_{22} + \alpha_{33}) \quad (5)$$

The anisotropy of the polarizability tensor is typically estimated by $\Delta\alpha$:[35]

$$\Delta\alpha = \left\{\frac{1}{2}[3\mathrm{Tr}(\boldsymbol{\alpha}^2) - (\mathrm{Tr}\boldsymbol{\alpha})^2]\right\}^{1/2} \quad (6)$$

All polarizabilities are reported in atomic units unless stated otherwise. Sources of error on the calculated polarizabilities are due to the incompleteness of both electronic correlation models and basis sets, and the limited accuracy of the atomic basin integration procedures.[42]

3. RESULTS AND DISCUSSION

3.1. Atomic and functional group polarizabilities in amino acid molecules

One of the main aims of our work is quantifying the contribution of individual atoms and, more importantly, of functional groups to specific optical properties, like the refractive index. Distributed atomic polarizabilities are particularly useful, because they enable reconstructing the polarizability of a functional group in a molecule by simple sum of the atomic tensors. Fig. 1 shows the polarizabilities for the twenty α-amino acids, in their zwitterionic configuration, calculated at the CAM-B3LYP/d-aug-cc-pVDZ level of theory. As already discussed,[38] atomic polarizabilities are extremely sensitive to the local chemical environment, being larger along the directions of covalently bonded atoms. For example, in the carboxylic groups, the polarizability ellipsoids of the oxygen atoms are stretched in the direction of the C–O bonds, because these

bonds are highly polarizable due to the π-bonding character and the large electronegativity difference between their atoms. In the carbonylic groups, the oxygen polarizability is approximately symmetrical about the C–O bond axis, unless involved in a hydrogen bond. Instead, the polarizability ellipsoid of oxydrilic oxygen atoms is slightly rotated due to the O–H bond. The hydrogen atoms have extremely prolate ellipsoids along the X–H bond direction, but overall their polarizabilities are very small due to their low electronic populations. Intramolecular hydrogen bonds increase the polarizability of H atoms, besides them being more positively charged, and modify the shape and orientation of the polarizability tensor of the hydrogen bond acceptor.

Fig. 1 also shows that each atom belonging to a functional group has very similar polarizabilities in all amino acids, suggesting a potentially good transferability. Table 1 gathers the average values for the diagonalized polarizability tensors of various functional groups. The standard deviation (SD) and the maximum absolute difference (MAD) from the mean are good indicators of the similarities. For the isotropic polarizability, α_{ISO}, SD and MAD are sufficiently small (less than 10% and 15% from the average values, respectively) for all but the methyl and methylenic functional groups. The anisotropy $\Delta\alpha$ is instead more variable. The worst outlier is methionine, for which the polarizability of the –CH_2– and –CH_3 groups is significantly larger than the average among all other amino acids. This difference is due to the highly polarizable sulfur atom, which increases the polarizability of all the atoms chemically bounded to it.

The average polarizabilities of the groups can be taken as the *transferable functional group* and used to estimate the electric susceptibility of a material, without carrying out a full quantum-

mechanical calculation. The polarizability ellipsoids for the transferable functional groups at the CAM-B3LYP/d-aug-cc-pVDZ level of theory are presented in Fig. 2. They were constrained to the idealized symmetry of the fragment by averaging the pertinent components of the tensor. For example, the polarizability of the carboxylate group was averaged in order to respect the ideal C_{2v} symmetry of the fragment.

Table 2 shows the calculated molecular polarizability tensors, with full *ab initio* treatments (at CAM-B3LYP and MP2 levels) or with the transferable-groups. As benchmark, we take the polarizabilities derived, using the Clausius-Mossotti equation, from experimental measurements of molar refraction in aqueous solution at $\lambda = 589\ nm$ and T = 25 °C.[43] The differences between experimental and calculated values are within 6%, a good result given that calculations do not account for wavelength dispersion or solvent effects.[44,45] Our results are also in good agreement with other additive models of dipole polarizabilities.[46]

The isotropic polarizabilities computed *via* the transferable groups (shown in Table 2 under the heading α_{iso}^{transf}) compare very well against the *ab initio* or the experimental values. For each amino acid, only small absolute differences occur, in the range of 1-3 *au* for most of the molecules, corresponding approximately to the propagated standard deviations of the transferable groups.

In order to confirm the validity of the transferable functional groups, we computed the polarizability of some molecules, for example β-alanine and α-aminoisobutyric acid, that contain the same functional groups but that are outside the set used to construct the database. The results

in Table 3 indicate that the transferable groups pass this test as well, again with good comparison against experimental values, when available.[47]

Our analysis enables to ascertain the role of each functional group in the buildup of optical properties. The linear susceptibility of a crystal is proportional to the unit-cell polarizability per unit cell-volume (a "polarizability density"), which is approximately an additive function. Therefore, the most promising functional groups and amino acid molecules are those that maximize their α/V ratio. In principle, the isotropic molecular polarizability and the molecular volume should correlate linearly.[22] Fig. 3(a) shows the linear regression between the calculated α_{ISO} and the molecular volume $V_{0.001au}$ (*i.e.* determined by a 0.001 au isosurface of electron density). The regression coefficient is 0.98. However, for some amino acids the calculated isotropic polarizabilities exceed the correlation, see Table 2 and Fig. 3(a). Cysteine, phenylalanine, tyrosine and tryptophan have in fact the larger $\alpha_{ISO}/V_{0.001au}$ ratio, see Fig. 3(b). For a proper estimation of the optical properties in the solid, one should consider the volume actually occupied by the molecule when embedded in the crystal, which depends on the packing ability, determined by the number of sites available for strong hydrogen bonding with the neighbors. Fig. 3(c) shows the polarizability density calculated as $Z\alpha_{ISO}/V_{unit-cell}$, where $V_{unit-cell}$ is the room-temperature unit cell volume and Z is the number of molecules per unit cell. The polarizability densities of glycine, tryptophan, phenylalanine and tyrosine are larger than those of the other molecules, addressing these amino acids as more promising for fabricating optical waveguides or other devices requiring high refractive index. Accurate experimental values are available only for few amino acids, whereas periodic DFT calculations, which we will present in details in a forthcoming paper, confirm highest refractive indices for

tryptophan, glycine, tyrosine and phenylalanine. With the exception of glycine, these molecules present aromatic rings, empirically well-known for large, though anisotropic, molecular polarizability. Even though high anisotropy is to be avoided in many optical applications, this is by no means a limitation on the use of the aromatic amino acids. In fact, molecules may pack in a crystal without alignment of the aromatic moieties, thus producing a rather isotropic susceptibility. The high $Z\alpha_{ISO}/V_{unit-cell}$ ratio for glycine is due to the relatively large contribution of the C_α atom to the molecular polarizability and the high packing density (of all known polymorphs, see Supporting Information) when compared to other amino acid crystals. In fact, as shown in Table 1, the C_α atom features the highest $\alpha_{ISO}/V_{0.001au}$ ratio of all functional groups, and in glycine, C_α counts more than in all other amino acids.

Analogously to the molecular quantities, the polarizability densities of the individual functional groups are useful parameters for the rational design of efficient opto-electronic molecules, especially concerning polymer-based optical devices, as the optical properties of their molecular subunits can be easily tunable by appropriate functionalization.[48]

3.2. Electron correlation and basis set effects

An important matter of debate is the role of electron correlation and basis-set completeness for the calculation of polarizabilities.[49] In order to investigate how much they affect for atomic polarizabilities, we have analyzed an isolated glycine molecule and three dimers (Fig. 4), with increasing amount of electron correlation and basis-set functions. In all dimers, the molecules are connected through one N–H···O hydrogen bond: one of them is a “head-to-tail” aggregation,

whereas the other two are “lateral” aggregations. Table 4 gathers the relevant features of molecular polarizability calculated at several levels, from Hartree-Fock (HF) to MP2 and CCSD with the augmented correlation-consistent basis sets. The isotropic polarizabilities, α_{ISO}, at CCSD and MP2 levels are *ca.* 10-15% larger than at the HF level. A similar trend is observed for $\Delta\alpha$. While α_{ISO} increases with the basis set size, the largest $\Delta\alpha$ occurs for the smallest aug-cc-pVDZ basis set.

Compared with CCSD, the truncated CI methods (CID and CISD) underestimate the magnitude of the polarizability tensors and their anisotropy, providing only a smaller increment compared with HF. On the other hand, CCSD and MP2 give quite comparable α_{ISO} and $\Delta\alpha$ (see Table 4) and the gap between the two methods is smaller for larger basis sets. The trend for the monomer is replicated by the dimer gly-gly-1 calculated at many intermediate levels of theory (CID, CISD and CCD) using the aug-cc-pVDZ basis set. The increasing correlation level has a very similar effect on either the donor or the acceptor molecules, whose polarizabilities are easily determined using the distributed atomic ones.

The highest level of approximation is the iterative introduction of triple or even quadruple excitations (CCSDT[50] or CCSDTQ[51] models). However, the trend observed for gly-gly-1 may suggest that high-order correlation is not likely to play a significant role for larger aggregates because, on going from CCD to CCSD, α_{ISO} increases less for the dimer than for the monomer. As concluded by Hammond *et al.*[8] for water clusters at various coupled-cluster levels of theory, triple or higher excitations are less significant as the number of molecules increases. Noteworthy, the calculation of amino acid aggregates is currently very challenging at the CCSDT level of

theory even with the smaller aug-cc-pVDZ basis set. While CCSDT/aug-cc-pVDZ calculations are feasible for the glycine monomer, this will likely not produce meaningful results due to the imbalance between a high-level correlation method and a small/medium size basis set.[52]

In light of these results, MP2 results as the most efficient level of theory, *i.e.* the one with largest accuracy/cost ratio, to estimate the electronic correlation effects on the distributed polarizabilities. Therefore, we have selected the MP2 level for benchmarking the various basis sets (see below) and DFT functionals (see next section).

Concerning the selection of a basis set, Table 5 lists the results at the HF and MP2 levels of theory for very large basis sets, up to quadruple-zeta quality and several levels of augmentation[53] within the Dunning family for the glycine monomer and the gly-gly-1 dimer. The number of diffuse functions is more important to achieve convergence than the valence splitting *X* for both α_{ISO} and $\Delta\alpha$: for the augmented basis sets, aug-cc-pV*X*Z, change in α_{ISO} and $\Delta\alpha$ is still noticeable on going from the double- to the triple-zeta quality sets, whereas the d-aug-cc-pV*X*Z series is already converged with the double-zeta quality basis set (*X* = D).

We can conclude that d-aug-cc-pVDZ is the ideal basis set to calculate the polarizabilities of the larger amino acid aggregates, again adopting a criterion of largest accuracy/cost ratio, where cost is here represented by the basis set rank.

Calculations of the glycine monomer and the gly-gly-1 dimer polarizabilities using Pople family of basis set are reported in the Supporting Information. The α_{ISO} convergence is extremely slow

mainly because the smaller Pople basis sets lack the additional diffuse functions present instead in the Dunning family. Only the largest Pople basis set, namely 6-311++G(3df,3pd), would be satisfactory but its rank is quite higher than d-aug-cc-pVDZ. For this reason, Pople basis sets are no further considered in our analysis.

3.3. Benchmarking of density functionals for distributed polarizabilities

Although the correct method to compute polarizabilities requires the explicit treatment of electronic correlation, for practical applications on large systems only DFT is feasible. Therefore, a functional is desirable that could provide results as close as possible to correlated calculations. We have evaluated the performances of the most popular density functionals for the calculation of distributed polarizabilities. The main features of the DFT schemes under investigation are described in the Supporting Information, classified according to Sousa *et al*.[54] As discussed in the previous section, MP2 is taken as benchmark. The comparisons refer to calculations performed using the d-aug-cc-pVTZ basis set, one of the most complete basis set applied in this study, certainly guaranteeing basis-set convergence as discussed in the previous section.

α_{ISO} and $\Delta\alpha$ for glycine calculated with the different density functionals are plotted in Fig. 5. The LSDA and GGA-based functionals underperform all the other DFT methods, with a clear tendency to overestimate both α_{ISO} and $\Delta\alpha$. The meta-GGA functionals provide some improvement, with errors ranging approximately from 5% to 13% with respect to the MP2/d-aug-cc-pVTZ benchmark. Hybrid functionals, which include part of exact exchange, generally

show good performance. Among them, the so-called long-range corrected ones, like CAM-B3LYP, or and the highly parameterized M06-2X and BMK functionals, predict the most accurate α_{ISO} and $\Delta\alpha$.

In view of these results and those presented in the previous section, we have selected the CAM-B3LYP/d-aug-cc-pVDZ level of theory to perform further calculations on dimers and small clusters. This is in keeping with the known limitations of "conventional" DFT (LSDA-, GGA-, M-GGA- and H-GGA-based functionals), that significantly overestimates (hyper)polarizabilities especially for systems presenting long-chain lengths.[55] In many cases, these drawbacks have been largely improved by applying long-range correction schemes[56-60] or highly parameterized functionals,[61] as confirmed by our results.

3.4. Hydrogen bond effects on the distributed polarizability of amino acid aggregates

The intermolecular interactions play a significant role for the susceptibilities of molecular crystals, typically enhanced by the cooperative effect of mutually induced polarization. In order to investigate this phenomenon from the point of view of distributed atomic polarizabilities, we selected ten hydrogen-bonded amino acid dimers, having N···O donor-acceptor distances in the range 2.68 – 2.97 Å, typical of medium-strength hydrogen bonds. The $–COO^-$ and $–NH_3^+$ group polarizabilities are summarized in Table 6, where they are also compared with the corresponding amino acid monomers.

The perturbation of the hydrogen bond linkage is quite significant in all cases. The polarizability of the $–NH_3^+$ donor is always increased, whereas that of the $–COO^-$ acceptor is either increased or decreased. There is no strict correlation with the N···O distance, given that interactions also occur amongst other atoms of the donor or acceptor molecules, even if not directly involved in the hydrogen bridge. The perturbation is highly anisotropic, because the aggregation occurs along the hydrogen bond direction, therefore all atoms in the donor or acceptor molecule increase their polarizability component along this direction.

Since molecular crystals feature in general only non-covalent intermolecular interactions, classical electrostatic models based on point dipoles have been adopted to estimate the crystal susceptibilities starting from the gas-phase molecular (hyper)polarizabilities.[62-65] It is important to check the consequences of neglecting the intermolecular interactions in the quantum-mechanical calculations, and accounting for them only through perturbative local field corrections. The distributed polarizability method is extremely useful in this respect, because it allows computing quantum-mechanically an entire aggregate and extracting the polarizabilities of individual molecules, after QTAIM partition. These quantities are then comparable with the approximated polarizabilities computed with the classical electrostatic perturbation of a gas-phase, isolated molecule. Munn and co-workers[66,67] derived the so-called rigorous local field theory (RLFT), in which the local field experienced by a molecule in a crystal is calculated with point-dipole approximation, by summing the fields arising from the surrounding dipoles in the crystal. The induced dipole moment due to the embedding of the isolated molecule in a crystal lattice equals the field-induced polarization of the isolated molecule. Using the QTAIM partition, the local electric field can be written as:

$$E_{j,local} = E_j + \sum_N \sum_\Omega \frac{\partial^2}{\partial r_i \partial r_j} (\boldsymbol{r} - \boldsymbol{R}_\Omega)^{-1} \mu_i(\Omega) \quad (7)$$

Where $E_{j,local}$ and E_j are the local and applied fields in direction j, respectively, and $\mu_i(\Omega)$ is the i component of the dipole moment vector of the basin Ω, computed for the molecule in isolation. The summations run over all atomic basins Ω within a given molecule *N*, and over all molecules in the crystal lattice. The components $\alpha_{ij}(\Omega)$ of the molecular polarizability are then perturbed and become $\alpha'_{ij}(\Omega)$ in the crystal:

$$\alpha'_{ij}(\Omega) = \lim_{\boldsymbol{E}\to 0} \frac{[E_{j,local} \cdot \alpha_{ij}(\Omega)]^{E_j} - [E_{j,local} \cdot \alpha_{ij}(\Omega)]^0}{E_j} \quad (8)$$

While the correctness of the RLFT approximation for the long-range interactions is out of discussion, the first coordination sphere requires more attention, because point electrostatic models may be inadequate. Therefore, we analyzed some glycine dimers, in order to test whether RLFT properly explains the polarizability changes. Two RLFT models have been employed and compared against the results of the "exact" QTAIM partition of the dimer. In RLFT1, each glycine molecule is approximated by a single point-dipole and polarizability at the center of mass of the molecule. In RLFT3, each glycine molecule is represented by three functional group point-dipoles and polarizabilities, each at the corresponding center of mass. Although the calculated electric field of Eqn. 7 is just a zero-order approximation, only few works[65, 68] have attempted to iterate the process, using the dipole moment of the polarized molecule to compute an improved approximation to the electric field. We used this iterative procedure, finding convergence on dipole moments and polarizabilities within 3-4 cycles (see Supporting Information). Table 7 and

Fig. 6 show the dipole moment for the glycine monomer and for the hydrogen-bond donor and acceptor molecules in the gly-gly-1 dimer. The head-to-tail aggregation induces an increased dipole moment, while its direction changes only slightly. The dipole moments from the QTAIM partitioning of the electron density are used as benchmarks, given that they come from a quantum-mechanical calculation of the entire dimer. The RLFT1 approximation [see Table 7 and Fig. 6(a)] does not distinguish the donor and the acceptor, of course because the two point dipoles and polarizability tensors are identical. This especially means underestimating the dipole moment of the donor. The RLFT3 model is instead able to differentiate the donor (with a larger dipole) from the acceptor, given that each group is treated separately. Nevertheless, RLFT3 is not completely correct because the dipole moment of the donor is overestimated with respect to the QTAIM results; see Table 7 and Fig. 6(b).

As indicated in Table 8, the RLFT1 and RLFT3 models yield similar polarizabilities, both of which overestimate the QTAIM results. Again, RLFT1 does not distinguish donor or acceptor, thus it does not predict the enhancement of the donor. On the other hand, RLFT3 overestimates the polarizability component along the hydrogen bond direction, resulting in too large anisotropies. This is not a failure of the distributed model, which is obviously more accurate than the model with just a global molecular polarizability. Instead, it is the manifestation of another problem, so far not much discussed in the literature, namely the volume contraction. In fact, the molecule in isolation is, by default, integrated within the isosurface $\rho(\boldsymbol{r}) = 0.001\ au$, which however corresponds to a much larger volume than the molecule in aggregation. In the gly-gly-1 example, this is particularly true along the hydrogen bond direction, being the other two directions anyway unconstrained. It seems therefore necessary to adopt a correction when using

gas-phase molecular polarizabilities in solid-state calculations: the molecular or group polarizabilities should be rescaled proportionally with the volume decrement.

In a small molecule such as glycine, the central or distributed polarizabilities methods do not differ substantially, whereas the distributed method should be more accurate in describing the anisotropies of larger molecules. In this sense, our results corroborate earlier findings for small molecules like urea and benzene,[64,69] whereas for a larger and more anisotropic molecule, nitroaniline, the spatial partitioning of the molecular response has been found to exert crucial influence on the crystal susceptibilities.[65]

In conclusion, our analysis suggests that the classical local field approximation could be improved in order to better estimate the polarizability increase of an aggregation (crystal), by taking into account a more accurate treatment of the short-range interactions. This will be the subject of further research in our group, implementing a hybrid scheme where the local interactions are accounted quantum-mechanically and included in the distributed atomic polarizabilities (thus automatically including also the volume contraction), whereas the long-range ones are evaluated with the classical local field approximation.

4. CONCLUSIONS

We have carried out a detailed analysis of the distributed atomic and functional group polarizabilities in amino acids and some of their aggregates. We focused on the contribution of

each functional group to the buildup of molecular/supramolecular properties and the effect of intermolecular interactions.

First, we demonstrated a very good transferability of the functional group polarizabilities. This enabled us to identify which group mostly contributes to the global dielectric constant of materials based on amino acids, which have recently attracted particular attention.[34] In particular, we found that the C_α atom provides a rather large optical density. In keeping with experimental evidence, another highly active group is the aromatic ring, which is also quite anisotropic (a feature to be carefully considered in the case where low or high birefringence is desirable). On the other hand, the sulfur atom, although itself quite polarizable, does not produce a very large molar refraction, because its atomic basin has a large volume. However, sulfur plays the role of enhancing the polarizabilities of all neighboring atoms, therefore it indirectly contributes to increasing the molecular and the overall crystal refraction.

Our study was also intended to identify the most quality/cost efficient method to calculate molecular and atomic polarizabilities. Careful analysis demonstrated that a hybrid DFT functional with long-range Coulomb attenuation, like CAM-B3LYP, gives results very close to those obtained with coupled-cluster techniques. As for the basis set, augmentation with diffuse functions is vital and even more important than valence splitting. Consequently, d-aug-cc-pVDZ is selected as the most efficient, at least for the series of molecules we investigated.

Another outcome of our analysis concerns the perturbation produced by medium strength intermolecular hydrogen bonds. A proper quantum-mechanical treatment of the first coordination is necessary to correctly estimate the effects of mutual polarization between two molecules. The classically adopted local field approximations, even in the more sophisticated distributed group

model, overestimate the polarizabilities of molecules in aggregation. The reason is that calculations in the gas-phase assume a too large volume for a molecule and therefore overestimate its polarizability in condensed matter. Based on these evidences, we will develop a new hybrid procedure for estimation of the crystal susceptibilities, meaning that the first coordination sphere of the molecule in the crystal is computed quantum-mechanically and that the semi-empirical local field perturbation is considered only for longer-range interactions.

The computational strategy outlined in this paper is a useful and effective tool for the rational design of optical organic materials, because it enables reasoning in terms of the transferable functional groups. Further studies are necessary to check the suitability of the strategy for other chemical systems.[70] Finally, this protocol may foster the development of models for the treatment of induction effects for force field simulations.

ASSOCIATED CONTENT

Supporting Information. Transferability of dipole moments in the amino acid series, molecular polarizability ellipsoids for some amino acids, polarizability density for different polymorphs and for the DL-forms, evaluation of the Pople family of basis set, atomic polarizability ellipsoids for the amino acid dimers. This material is available free of charge via the Internet at http://pubs.acs.org.

AUTHOR INFORMATION

Corresponding Authors

*E-mail: leonardo.rezende@dcb.unibe.ch, piero.macchi@dcb.unibe.ch

Notes

The authors declare no competing financial interest.

ACKNOWLEDGMENT

The authors thank Prof. B. Champagne for the critical reading of the manuscript prior to its submission. This work was supported by the Swiss National Science Foundation, Project No. 141271.

REFERENCES

(1) Maroulis, G. (Ed.) *Computational Aspects of Electric Polarizability Calculations: Atoms, Molecules and Clusters*; IOS Press: Amsterdam, The Netherlands, 2006.

(2) Nalwa, H. S.; Miyata, S. (Eds.) *Nonlinear Optics of Organic Molecules and Polymers*; CRC Press: Boca Raton, USA, 1996.

(3) Chemla, D. S.; Zyss, J. (Eds.) *Nonlinear Optical Properties of Organic Molecules and Crystals*; Academic Press: London, U. K., 1987.

(4) Karna, S. P. Electronic and Nonlinear Optical Materials: The Role of Theory and Modeling. *J. Phys. Chem. A* **2000**, *104*, 4671-4673.

(5) Champagne, B.; Bishop, D. M. Calculations of Nonlinear Optical Properties for the Solid State. *Adv. Chem. Phys.* **2003**, *126*, 41-92.

(6) Orlando, R.; Lacivita, V.; Bast, R.; Ruud, K. Calculation of the First Static Hyperpolarizability Tensor of Three-Dimensional Periodic Compounds with a Local Basis Set: A Comparison of LDA, PBE, PBE0, B3LYP and HF Results. *J. Chem. Phys.* **2010**, *132*, 244106.

(7) Balakina, M. Y.; Fominykh, O. D. The Quantum-Chemical Study of Small Clusters of Organic Chromophores: Topological Analysis and Nonlinear Optical Properties. *Int. J. Quantum Chem.* **2008**, *108*, 2678-2692.

(8) Hammond, J. R.; Govind, N.; Kowalski, K.; Autschbach, J.; Xantheas, S. S. Accurate Dipole Polarizabilities for Water Clusters *n* = 1-12 at the Coupled-Cluster Level of Theory and Benchmarking of Various Density Functionals. *J. Chem. Phys.* **2009**, *131*, 214103.

(9) Marenich, A. V.; Cramer, C. J.; Truhlar, D. G. Reduced and Quenched Polarizabilities of Interior Atoms in Molecules. *Chem. Sci.* **2013**, *4*, 2349-2356.

(10) Bader, R. F. W.; Larouche, A.; Gatti, C.; Carroll, M. T.; MacDougall, P. J.; Wiberg, K. B. Properties of Atoms in Molecules: Dipole Moments and Transferability of Properties. *J. Chem. Phys.* **1987**, *87*, 1142-1152.

(11) Bader, R. F. W.; Keith, T. A.; Gough, K. M.; Laidig, K. E. Properties of Atoms in Molecules: Additivity and Transferability of Group Polarizabilities. *Mol. Phys.* **1992**, *75*, 1167-1189.

(12) Bader, R. F. W.; Matta, C. F. Properties of Atoms in Crystals: Dielectric Polarization. *Int. J. Quantum Chem.* **2001**, *85*, 592-607.

(13) Applequist, J. An Atom Dipole Interaction Model for Molecular Optical Properties. *Acc. Chem. Res.* **1977**, 79-85.

(14) Miller, K. J. Additivity Methods in Molecular Polarizability. *J. Am. Chem. Soc.* **1990**, *112*, 8533-8542.

(15) Stout, J. M.; Dykstra, C. E. A Distributed Model of the Electrical Response of Organic Molecules. *J. Phys. Chem. A*, **1998**, *102*, 1576-1582.

(16) van Duijnen, P. Th.; Swart, M. Molecular and Atomic Polarizabilities: Thole's Model Revisited. *J. Phys. Chem. A*, **1998**, *102*, 2399-2407.

(17) Zhou, T.; Dykstra, C. E. Additivity and Transferability of Atomic Contributions to Molecular Second Dipole Hyperpolarizabilities. *J. Phys. Chem. A*, **2000**, *104*, 2204-2210.

(18) Maple, J. R.; Ewig, C. S. An Ab Initio Procedure for Deriving Atomic Polarizability Tensors in Molecules. *J. Chem. Phys.* **2001**, *115*, 4981-4988.

(19) Ewig, C. S.; Waldman, M.; Maple, J. R. Ab Initio Atomic Polarizability Tensors for Organic Molecules. *J. Phys. Chem. A*, **2002**, *106*, 326-334.

(20) in het Panhuis, M.; Munn, R. W.; Popelier, P. L. A. Distributed Polarizability Analysis for para-Nitroaniline and meta-Nitroaniline: Functional Group and Charge-Transfer Contributions. *J. Chem. Phys.* **2004**, *120*, 11479-11486.

(21) Geldof, D.; Krishtal, A.; Geerlings, P.; Van Alsenoy, C. Partitioning of Higher Multipole Polarizabilities: Numerical Evaluation of Transferability. *J. Phys. Chem. A*, **2011**, *115*, 13096-13103.

(22) Laidig, K. E.; Bader, R. F. W. Properties of Atoms in Molecules: Atomic Polarizabilities. *J. Chem. Phys.* **1990**, *93*, 7213-7224.

(23) Jansen, G.; Hättig, C.; Hess, B. A.; Ángyán, J. G. Intermolecular Interaction Energies by Topologically Partitioned Electric Properties. I. Electrostatic and Induction Energies in One-Centre and Multicentre Multipole Expansions. *Mol. Phys.* **1996**, *88*, 69-92.

(24) Hättig, C.; Jansen, G.; Hess, B. A.; Ángyán, J. G. Intermolecular Interaction Energies by Topologically Partitioned Electric Properties. II. Dispersion Energies in One-Centre and Multicentre Multipole Expansions. *Mol. Phys.* **1997**, *91*, 145-160.

(25) in het Panhuis, M.; Popelier, P. L. A.; Munn, R. W.; Ángyán, J. G. Distributed Polarizability of the Water Dimer: Field-Induced Charge Transfer Along the Hydrogen Bond. *J. Chem. Phys.* **2001**, *114*, 7951-7961.

(26) Stone, A. J.; Hättig, C.; Jansen, G.; Ángyán, J. G. Transferability of Topologically Partitioned Polarizabilities: the Case of n-Alkanes. *Mol. Phys.* **1996**, *89*, 595-605.

(27) Keith, T. A. In *The Quantum Theory of Atoms in Molecules*; Matta, C. F.; Boyd, R. J.; Wiley-VCH Verlag GmbH & Co. KGaA: Weinheim, Germany, 2007, pp 61-94.

(28) Krawczuk, A.; Pérez, D.; Macchi, P. PolaBer: A Program to Calculate and Visualize Distributed Atomic Polarizabilities Based on Electron Density Partitioning. *J. Appl. Cryst.* **2014**, *47*, 1452-1458.

(29) Stone, A. J. Distributed Polarizabilities. *Mol. Phys.* **1985**, *56*, 1065-1082.

(30) Le Sueur, C. R.; Stone, A. J. Practical Schemes for Distributed Polarizabilities. *Mol. Phys.* **1993**, *78*, 1267-1291.

(31) Stone, A. J.; Alderton, M. Distributed Multipole Analysis: Methods and Applications. *Mol. Phys.* **2002**, *100*, 221-233.

(32) Krishtal, A.; Senet, P.; Yang, M.; Van Alsenoy, C. A Hirshfeld Partitioning of Polarizabilities of Water Clusters. *J. Chem. Phys.* **2006**, *125*, 034312.

(33) Bultinck, P.; Van Alsenoy, C.; Ayers, P. W.; Carbó-Dorca, R. Critical Analysis and Extension of the Hirshfeld Atoms in Molecules. *J. Chem. Phys.* **2007**, *126*, 144111.

(34) Chimpri, A. S.; Gryl, M.; Dos Santos, L. H. R.; Krawczuk, A.; Macchi, P. Correlation Between Accurate Electron Density and Linear Optical Properties in Amino Acid Derivatives: L-Histidinium Hydrogen Oxalate. *Cryst. Growth Des.* **2013**, *13*, 2995-3010.

(35) Bonin, K. D.; Kresin, V. V. *Electric-dipole Polarizabilities of Atoms, Molecules and Clusters*; World Scientific Publishing Co. Pte. Ltd.: London, U.K., 1962.

(36) Frisch, M. J.; Trucks, G. W.; Schlegel, H. B.; Scuseria, G. E.; Robb, M. A.; Cheeseman, J. R.; Montgomery, J. A., Jr.; Vreven, T.; Kudin, K. N.; Burant, J. C. et al. Gaussian 09; Gaussian, Inc.: Wallingford, CT, 2009.

(37) Keith, T. A. AIMAll, Version 14.04.17; TK Gristmill Software: Overland Park, KS, USA, 2014, aim.tkgristmill.com.

(38) Krawczuk-Pantula, A.; Pérez, D.; Stadnicka, K.; Macchi, P. Distributed Atomic Polarizabilities from Electron Density. I. Motivations and Theory. *Trans. Am. Cryst. Ass.* **2011**, *42*, 1-25.

(39) Bishop, D. M.; Kirtman, B. A Perturbation Method for Calculating Vibrational Dynamic Dipole Polarizabilities and Hyperpolarizabilities. *J. Chem. Phys.* **1991**, *95*, 2646-2658.

(40) Bishop, D. M.; Kirtman, B. Compact Formulas for Vibrational Dynamic Dipole Polarizabilities and Hyperpolarizabilities. *J. Chem. Phys.* **1992**, *97*, 5255-5256.

(41) Nye, J. F. *Physical Properties of Crystals: Their Representation by Tensors and Matrices*; Oxford University Press: Oxford, U.K., 1985.

(42) Biegler-König, F. W.; Bader, R. F. W.; Tang, T. H. Calculation of the Average Properties of Atoms in Molecules. II. *J. Comput. Chem.* **1982**, *3*, 317-328.

(43) McMeekin, T. L.; Groves, M. L.; Hipp, N. J. In *Amino Acids and Serum Proteins*; Stekol, J; Advances in Chemistry; American Chemical Society: Washington, USA, 1964, pp 54-66.

(44) Balakina, M. Y.; Nefediev, S. E. Solvent Effect on Geometry and Non-linear Optical Response of Conjugated Organic Molecules. *Int. J. Quantum Chem.* **2006**, *106*, 2245-2253.

(45) Reis, H. Problems in the Comparison of Theoretical and Experimental Hyperpolarizabilities Revisited. *J. Chem. Phys.* **2006**, *125*, 014506.

(46) Kassimi, N. E.-B.; Thakkar, A. J. A Simple Additive Model for Polarizabilities: Application to Amino Acids. *Chem. Phys. Lett.* **2009**, *472*, 232-236.

(47) Khanarian, G.; Moore, W. J. The Kerr Effect of Amino Acids in Water. *Aust. J. Chem.* **1980**, *33*, 1727-1741.

(48) Ma, H.; Jen, A. K.-Y.; Dalton, L. R. Polymer-Based Optical Waveguides: Materials, Processing, and Devices. *Adv. Mat.* **2002**, *14*, 1339-1365.

(49) Medved, M.; Champagne, B.; Noga, J.; Perpète, E. A. In *Computational Aspects of Electric Polarizability Calculations: Atoms, Molecules and Clusters*; Maroulis, G. IOS Press: Amsterdam, The Netherlands, 2006, pp 17-31.

(50) Scuseria, G. E.; Schaefer III, H. F. A New Implementation of the Full CCSDT Model for Molecular Electronic Structure. *Chem. Phys. Lett.* **1988**, *152*, 382-386.

(51) Kucharski, S. A.; Bartlett, R. J. The Coupled-Cluster Single, Double, Triple and Quadruple Excitation Method. *J. Chem. Phys.* **1992**, *97*, 4282-4288.

(52) Helgaker, T.; Ruden, T. A.; Jørgensen, P.; Olsen, J.; Klopper, W. A Priori Calculation of Molecular Properties to Chemical Accuracy. *J. Phys. Org. Chem.* **2004**, *17*, 913-933.

(53) Papajak, E.; Zheng, J.; Xu, X.; Leverentz, H. R.; Truhlar, D. G. Perspectives on Basis Sets Beautiful: Seasonal Plantings of Diffuse Basis Functions. *J. Chem. Theory Comput.* **2011**, *7*, 3027-3034.

(54) Sousa, S. F.; Fernandes, P. A.; Ramos, M. J. General Performance of Density Functionals. *J. Phys. Chem. A*, **2007**, *111*, 10439-10452.

(55) de Wergifosse, M.; Champagne, B. Electron Correlation Effects on the First Hyperpolarizability of Push-Pull π-Conjugated Systems. *J. Chem. Phys.* **2011**, *134*, 074113.

(56) Yanai, T.; Tew, D. P.; Handy, N. C. A New Hybrid Exchange-Correlation Functional Using the Coulomb-Attenuating Method (CAM-B3LYP). *Chem. Phys. Lett.* **2004**, *393*, 51-57.

(57) Song, J.-W.; Watson, M. A.; Sekino, H.; Hirao, K. Nonlinear Optical Property Calculations of Polyynes with Long-Range Corrected Hybrid Exchange-Correlation Functionals. *J. Chem. Phys.* **2008**, *129*, 024117.

(58) Sekino, H.; Maeda, Y.; Kamiya, M.; Hirao, K. Polarizability and Second Hyperpolarizability Evaluation of Long Molecules by the Density Functional Theory with Long-Range Correction. *J. Chem. Phys.* **2007**, *126*, 014107.

(59) Kamiya, M.; Sekino, H.; Tsuneda, T.; Hirao, K. Nonlinear Optical Property Calculations by the Long-Range-Corrected Coupled-Perturbed Kohn-Sham Method. *J. Chem. Phys.* **2005**, *122*, 234111.

(60) Iikura, H.; Tsuneda, T.; Yanai, T.; Hirao, K. Long-Range Correction Scheme for Generalized-Gradient-Approximation Exchange Functionals. *J. Chem. Phys.* **2001**, *115*, 3540-3544.

(61) Zhao, Y.; Truhlar, D. G. The M06 Suite of Density Functionals for Main Group Thermochemistry, Thermochemical Kinetics, Noncovalent Interactions, Excited States, and Transition Elements: Two New Functionals and Systematic Testing of Four M06-Class Functionals and 12 other Functionals. *Theor. Chem. Acc.* **2008**, *120*, 215-241.

(62) Chemla, D. S.; Oudar, J. L.; Jerphagnon, J. Origin of the Second-Order Optical Susceptibilities of Crystalline Substituted Benzene. *Phys. Rev. B*, **1975**, *12*, 4534-4546.

(63) Dunmur, D. A. The Local Electric Field in Anisotropic Molecular Crystals. *Mol. Phys.* **1972**, *23*, 109-115.

(64) Reis, H.; Raptis, S.; Papadopoulos, M. G.; Janssen, R. H. C.; Theodorou, D. N.; Munn, R. W. Calculation of Macroscopic First- and Third-Order Optical Susceptibilities for the Benzene Crystal. *Theor. Chem. Acc.* **1998**, *99*, 384-390.

(65) Reis, H.; Papadopoulos, M. G.; Calaminici, P.; Jug, K.; Köster, A. M. Calculation of Macroscopic Linear and Nonlinear Optical Susceptibilities for the Naphthalene, Anthracene and meta-Nitroaniline Crystals. *Chem. Phys.* **2000**, *261*, 359-371.

(66) Munn, R. W. Electric Dipole Interactions in Molecular Crystals. *Mol. Phys.* **1988**, *64*, 1-20.

(67) Cummins, P. G.; Dunmur, D. A.; Munn, R. W.; Newham, R. J. Applications of the Ewald Method. I. Calculation of Multipole Lattice Sums. *Acta Cryst. Sect. A*, **1976**, *32*, 847-853.

(68) Spackman, M. A.; Munshi, P.; Jayatilaka, D. The Use of Dipole Lattice Sums to Estimate Electric Fields and Dipole Moment Enhancement in Molecular Crystals. *Chem. Phys. Lett.* **2007**, *443*, 87-91.

(69) Reis, H.; Papadopoulos, M. G.; Munn, R. W. Calculation of Macroscopic First-, Second-, and Third-Order Optical Susceptibilities for the Urea Crystal. *J. Chem. Phys.* **1998**, *109*, 6828-6838.

(70) Macchi, P.; Krawczuk, A. The Polarizability of Organometallic Bonds. *Comput. Theoret. Chem.* **2015**, *1053*, 165-172.

Table 1. Average values of functional group polarizabilities in the 20 amino acids. Standard deviations (SD) and maximum absolute differences (MAD) from the mean for polarizability features (*au*) are given. In parenthesis are the amino acids for which the maximum differences occur. Calculations are at the CAM-B3LYP and MP2 levels of theory with the d-aug-cc-pVDZ basis set.[a]

	Average		MAD	
	CAM-B3LYP	MP2	CAM-B3LYP	MP2
COO^-				
α_{11}	14.9 ± 0.5	15.4 ± 0.6	1.6 (arg)	1.6 (arg)
α_{22}	26.9 ± 0.8	28 ± 1	1.8 (tyr)	1.6 (arg)
α_{33}	28.8 ± 0.9	29.9 ± 0.9	1.6 (his)	1.9 (gly)
α_{iso}	23.5 ± 0.5	24.4 ± 0.5	1.2 (arg)	1.1 (arg)
$\Delta\alpha$	13.1 ± 0.7	13.7 ± 0.8	1.3 (try)	1.3 (tyr)
$\alpha_{iso}/V_{0.001au}$	0.073	0.073	…	…
NH_3^+				
α_{11}	7.3 ± 0.8	7.4 ± 0.3	1.9 (cys)	0.8 (gly)
α_{22}	8 ± 1	8.6 ± 0.9	2.7 (his)	3.4 (his)
α_{33}	15 ± 1	14.5 ± 0.8	2.8 (cys)	1.5 (cys)
α_{iso}	10.1 ± 0.9	10.2 ± 0.3	2.3 (phe)	0.9 (cys)
$\Delta\alpha$	6.8 ± 0.9	6.6 ± 0.9	1.7 (his)	1.6 (asp)
$\alpha_{iso}/V_{0.001au}$	0.062	0.062	…	…
$C\alpha$				
α_{11}	4.3 ± 0.3	4.3 ± 0.3	0.7 (try)	0.7 (pro)
α_{22}	7.8 ± 0.7	7.5 ± 0.7	2.0 (arg)	1.9 (arg)
α_{33}	10 ± 1	10 ± 1	3 (arg)	3 (arg)
α_{iso}	7.4 ± 0.3	7.3 ± 0.3	0.6 (thr)	0.5 (tyr)
$\Delta\alpha$	5 ± 1	5 ± 1	3 (arg)	3 (arg)
$\alpha_{iso}/V_{0.001au}$	0.15	0.15	…	…
CH_3				
α_{11}	11.7 ± 0.4	11.5 ± 0.5	0.8 (ileu)	0.7 (met)
α_{22}	12.2 ± 0.3	12.2 ± 0.4	0.4 (val)	0.7 (ileu)
α_{33}	17 ± 2	17 ± 2	5 (met)	7 (met)
α_{iso}	13.6 ± 0.7	13.6 ± 0.8	1.4 (met)	2.0 (met)
$\Delta\alpha$	5 ± 2	5 ± 2	4 (met)	6 (met)
$\alpha_{iso}/V_{0.001au}$	0.062	0.062	...	...

$C(sp^3)H_2$				
α_{11}	8.5 ± 0.9	8.5 ± 0.7	2.1 (cys)	1.6 (gly)
α_{22}	10 ± 1	10 ± 1	3 (tyr)	3 (tyr)
α_{33}	14 ± 2	14 ± 2	5 (met)	6 (met)
α_{iso}	11.0 ± 0.8	11 ± 1	1.6 (tyr)	2 (asp)
$\Delta\alpha$	5 ± 2	5 ± 2	5 (met)	5 (met)
$\alpha_{iso}/V_{0.001au}$	0.073	0.073	...	...
$C(sp^3)H$				
α_{11}	7.7 ± 0.9	7.8 ± 0.7	2.0 (pro)	1.9 (thr)
α_{22}	9.3 ± 0.6	9.3 ± 0.5	1.4 (cys)	1.1 (asp)
α_{33}	11 ± 1	11 ± 1	4 (arg)	4 (arg)
α_{iso}	9.5 ± 0.6	9.5 ± 0.5	1.5 (thr)	1.2 (thr)
$\Delta\alpha$	3 ± 1	3 ± 1	4 (arg)	3 (arg)
$\alpha_{iso}/V_{0.001au}$	0.10	0.10	…	…
OH				
α_{11}	5.3 ± 0.1	5.5 ± 0.1	0.2 (thr)	0.2 (asp)
α_{22}	6.5 ± 0.6	6.4 ± 0.5	0.9 (tyr)	0.8 (glu)
α_{33}	13 ± 2	14 ± 2	3 (tyr)	3 (tyr)
α_{iso}	8.6 ± 0.4	8.7 ± 0.4	0.7 (tyr)	0.6 (ser)
$\Delta\alpha$	8 ± 2	8 ± 2	3 (tyr)	3 (tyr)
$\alpha_{iso}/V_{0.001au}$	0.058	0.058	...	...
C=O				
α_{11}	7.2 ± 0.3	7.3 ± 0.3	0.4 (glu)	0.4 (asn)
α_{22}	12.7 ± 0.9	13 ± 1	1.7 (asn)	2 (glu)
α_{33}	17 ± 1	17 ± 1	2 (gln)	2 (asp)
α_{iso}	12.4 ± 0.4	12.6 ± 0.4	0.6 (gln)	0.6 (gln)
$\Delta\alpha$	8.9 ± 0.9	9 ± 1	1.4 (asp)	1 (asp)
$\alpha_{iso}/V_{0.001au}$	0.072	0.072	…	…
$N(sp^2)H_2$				
α_{11}	7.9 ± 0.5	8.3 ± 0.6	0.6 (gln)	0.7 (gln)
α_{22}	9.1 ± 0.5	9.2 ± 0.6	0.8 (arg)	0.9 (arg)
α_{33}	17.4 ± 0.9	18.0 ± 0.9	1.6 (arg)	1.6 (arg)
α_{iso}	11.5 ± 0.4	11.8 ± 0.4	0.5 (arg)	0.6 (arg)
$\Delta\alpha$	8.9 ± 0.9	8.9 ± 0.9	1.3 (arg)	1.3 (arg)
$\alpha_{iso}/V_{0.001au}$	0.067	0.067	…	…
$(C_6)_{\text{phenyl ring}}{}^{b}$				
α_{11}	29.9 ± 0.7	30.9 ± 0.9	1.1 (try)	1.5 (try)
α_{22}	51 ± 3	55 ± 1	3 (phe)	1 (phe)
α_{33}	72 ± 5	77 ± 4	5 (phe)	4 (tyr)
α_{iso}	51 ± 2	54 ± 1	3 (phe)	2 (try)
$\Delta\alpha$	36 ± 5	39 ± 3	5 (phe)	4 (tyr)

$\alpha_{iso}/V_{0.001au}$ S	0.11	0.11	…	…
α_{11}	14 ± 1	15 ± 1	…	…
α_{22}	17.6 ± 0.1	17.8 ± 0.2	…	…
α_{33}	24.2 ± 0.8	24.7 ± 0.2	…	…
α_{iso}	18.8 ± 0.8	19.1 ± 0.6	…	…
$\Delta\alpha$	8.6 ± 0.4	8.8 ± 0.9	…	…
$\alpha_{iso}/V_{0.001au}$	0.089	0.089	…	…

[a] $V_{0.001au}$ denotes the functional-group volume defined by an electron density isosurface of 0.001 *au*. SD and MAD values relative to the $\alpha_{iso}/V_{0.001au}$ ratio are omitted as they are very small.

[b] The transferable features for the phenyl ring were calculated neglecting the H atoms as this allows one to export the group for molecules containing more than one substituent in the ring. The polarizability of the H atoms is anyway negligible compared to the entire group.

Table 2. Diagonalized tensor components for the static dipole polarizability (*au*) of the amino acids calculated at CAM-B3LYP and MP2 levels of theory using the d-aug-cc-pVDZ basis set.

	CAM-B3LYP/d-aug-cc-pVDZ						MP2/d-aug-cc-pVDZ						Exp.[a]
	α_{11}	α_{22}	α_{33}	α_{iso}	$\Delta\alpha$	α_{iso}^{transf}	α_{11}	α_{22}	α_{33}	α_{iso}	$\Delta\alpha$	α_{iso}^{transf}	α_{iso}
Glycine	35.78	49.31	57.88	47.66	19.30	45 ± 1	36.26	50.35	57.77	48.13	18.92	46 ± 1	44.3 ± 0.6
Alanine	47.32	58.45	65.12	56.96	15.58	57 ± 1	47.42	59.44	64.89	57.25	15.48	58 ± 1	55.9 ± 0.7
Valine	72.23	80.23	86.05	79.50	12.02	80 ± 2	72.10	80.05	86.85	79.67	12.79	81 ± 1	81.5 ± 0.4
Isoleucine	81.84	91.34	101.33	91.50	16.88	91 ± 2	82.33	91.31	102.10	91.91	17.15	92 ± 2	95.2 ± 0.6
Leucine	86.17	91.70	97.43	91.77	9.75	91 ± 2	86.94	92.12	98.04	92.37	9.62	92 ± 2	94.5 ± 0.4
Serine	53.06	63.82	69.10	62.00	14.16	63 ± 1	53.14	64.35	69.09	62.19	14.19	64 ± 1	61.2 ± 0.4
Threonine	61.73	78.13	79.36	73.07	17.05	72 ± 2	62.19	78.77	80.27	73.74	17.38	73 ± 1	73.7 ± 0.4
Proline	64.66	73.55	81.65	73.29	14.72	76 ± 2	64.98	74.31	82.39	73.89	15.09	77 ± 2	73.5 ± 0.4
Aspartic acid	59.04	75.52	86.75	73.77	24.14	75 ± 2	59.71	76.54	87.06	74.44	23.90	76 ± 1	…
Glutamic acid	74.12	89.84	95.38	86.45	19.10	86 ± 2	74.46	91.01	95.89	87.12	19.45	87 ± 2	90.4 ± 0.4
Lysinium	81.57	94.85	118.23	98.22	32.15	101 ± 2	81.60	95.15	117.13	97.96	31.06	102 ± 2	101.2 ± 0.5[b]
Arginine	99.74	115.89	138.52	118.05	33.74	115 ± 2	101.16	117.81	140.67	119.88	34.36	116 ± 2	115.6 ± 0.2
Asparagine	70.49	77.53	89.90	79.31	17.02	78 ± 2	71.28	77.83	91.93	80.35	18.28	80 ± 1	79.8 ± 0.7
Glutamine	82.54	93.28	95.43	90.42	11.96	89 ± 2	83.02	94.91	95.94	91.29	12.44	91 ± 2	91.2 ± 0.6
Cysteine	57.26	71.38	87.13	77.92	25.88	76 ± 1	63.29	76.78	94.85	78.31	27.43	77 ± 1	…
Methionine	81.92	97.99	126.78	102.23	39.37	100 ± 2	82.52	98.49	128.26	103.09	40.21	101 ± 2	102.1 ± 0.1
Tryptophan	104.20	161.57	197.90	154.56	81.82	156 ± 2	106.51	161.07	201.39	156.32	82.48	150 ± 2	157.8 ± 0.5
Phenylalanine	96.19	122.64	150.18	123.00	46.76	119 ± 2	97.77	124.15	151.63	124.52	46.64	123 ± 2	122.9 ± 0.3
Tyrosine	95.25	132.60	153.86	127.24	51.39	127 ± 2	97.10	133.03	154.95	128.36	50.59	130 ± 2	…
Histidine	73.12	104.25	127.63	101.67	47.37	99 ± 1	74.28	105.47	128.48	102.75	47.12	100 ± 1	102.6 ± 0.4

[a] Experimental values extracted from the molar refractions, measured in aqueous solution at λ = 589 nm and 25 °C, using the Clausius-Mossotti equation, from ref. 43.
[b] Reported value for lysine.

Table 3. Diagonalized tensor components for the static dipole polarizability (*au*) of β-alanine and α-aminoisobutyric acid, calculated *ab initio*, at the CAM-B3LYP/d-aug-cc-pVDZ level of theory, and using the transferable-group treatment.

	CAM-B3LYP/d-aug-cc-pVDZ					Transferable-group treatment					Exp.[a]
	α_{11}	α_{22}	α_{33}	α_{iso}	$\Delta\alpha$	α_{11}	α_{22}	α_{33}	α_{iso}	$\Delta\alpha$	α_{iso}
β-alanine	44.06	53.92	65.86	54.61	18.91	45.24	53.04	67.62	55.30	19.67	...
α-aminoisobutyric acid	56.21	66.23	69.68	64.04	12.11	61.79	68.65	74.35	68.26	10.89	67.34

[a] Experimental value extracted from molar refraction, measured in aqueous solution at λ = 578 nm, using the Clausius-Mossotti equation, from ref. 47.

Table 4. Static dipole polarizabilities (*au*) of the glycine monomer and the gly-gly dimers. The isotropic polarizability (α_{ISO}) and the anisotropy of polarizability ($\Delta\alpha$) are reported for the aug-cc-pVDZ, aug-cc-pVTZ and d-aug-cc-pVDZ basis sets using a variety of methods. In the dimers, the polarizabilities for the hydrogen bond donor and acceptor molecules are reported. Due to computational costs, full series of correlated calculation was performed only for gly-gly-1 with aug-cc-pVDZ basis set.

		α_{ISO}						$\Delta\alpha$					
	Method	aug-cc-pVDZ		aug-cc-pVTZ		d-aug-cc-pVDZ		aug-cc-pVDZ		aug-cc-pVTZ		d-aug-cc-pVDZ	
monomer	HF	41.29		41.63		41.80		13.86		13.67		13.72	
	CID	43.31		43.32		43.89		15.67		15.66		15.74	
	CISD	43.44		43.39		44.03		16.09		15.75		15.91	
	CCD	45.24		45.27		45.89		16.89		17.04		17.22	
	CCSD	46.70		46.45		47.38		19.10		18.48		18.87	
	MP2	47.38		47.75		48.13		19.15		18.96		18.92	
		donor	acceptor	donor	acceptor	donor	acceptor	donor	acceptor	donor	acceptor	donor	acceptor
gly-gly-1	HF	41.54	40.49	42.03	40.65	42.01	40.62	14.88	16.17	15.17	16.30	14.88	16.09
	CID	43.00	41.66	…	…	43.53	41.90	16.65	17.70	…	…	16.46	17.47
	CISD	43.03	41.69	…	…	43.56	41.93	16.71	17.71	…	…	16.50	17.52
	CCD	45.62	43.96	…	…	…	…	18.72	19.52	…	…	…	…
	CCSD	46.88	45.11	…	…	…	…	20.35	21.37	…	…	…	…
	MP2	47.73	45.75	48.17	45.83	48.51	46.04	20.51	21.37	20.53	21.37	20.47	21.31
gly-gly-2	HF	42.41	41.36	42.63	41.52	42.83	41.67	16.63	17.44	16.17	17.20	16.40	17.17
	MP2	49.46	47.44	49.63	47.62	50.13	47.88	22.72	22.93	22.26	22.69	22.38	22.62
gly-gly-3	HF	41.91	40.84	42.27	41.02	42.36	41.15	9.51	16.80	9.33	16.63	9.14	16.95
	MP2	48.92	46.82	49.39	46.32	49.46	47.05	13.41	22.29	13.49	21.76	13.12	22.11

Table 5. Static dipole polarizabilities and their anisotropies (*au*) for the glycine monomer and the gly-gly-1 dimer at HF and MP2 levels of theory with the Dunning family of basis sets. In the dimer, the polarizabilities for the hydrogen bond donor and acceptor molecules are reported.

			α_{ISO}				$\Delta\alpha$			
	Basis set	Rank	HF		MP2		HF		MP2	
monomer	cc-pVDZ	95	32.63		35.95		12.72		16.63	
	cc-pVTZ	220	37.06		41.03		13.26		17.60	
	cc-pVQZ	425	39.29		43.92		13.65		18.40	
	m-aug-cc-pVDZ	115	38.27		44.16		14.01		19.17	
	m-aug-cc-pVTZ	240	40.11		45.84		14.15		19.37	
	m-aug-cc-pVQZ	445	40.88		46.59		13.99		19.21	
	aug-cc-pVDZ	160	41.29		47.38		13.86		19.15	
	aug-cc-pVTZ	345	41.63		47.75		13.67		18.96	
	aug-cc-pVQZ	630	41.71		47.75		13.66		18.84	
	d-aug-cc-pVDZ	225	41.80		48.13		13.72		18.92	
	d-aug-cc-pVTZ	470	41.80		47.97		13.72		18.85	
	d-aug-cc-pVQZ	835	41.75		47.81		13.67		18.81	
			donor	acceptor	donor	acceptor	donor	acceptor	donor	acceptor
gly-gly-1	cc-pVDZ	190	33.40	32.54	36.77	35.65	15.56	12.60	20.42	16.87
	cc-pVTZ	440	37.40	36.99	41.45	40.99	16.40	13.93	21.69	18.76
	m-aug-cc-pVDZ	230	38.59	37.52	44.69	42.64	14.02	14.96	19.55	20.03
	m-aug-cc-pVTZ	480	40.31	39.32	46.25	44.30	14.66	15.88	20.41	21.05
	aug-cc-pVDZ	320	41.54	40.49	47.73	45.75	14.88	16.17	20.51	21.37
	aug-cc-pVTZ	690	42.03	40.65	48.17	45.83	15.17	16.30	20.53	21.37
	d-aug-cc-pVDZ	450	42.01	40.62	48.51	46.04	14.88	16.09	20.47	21.31

Table 6. Static dipole polarizabilities and their anisotropies (*au*) for the hydrogen-bonded carboxylate and ammonium groups in the amino acid dimers and comparison with the corresponding values for the monomers at the CAM-B3LYP/d-aug-cc-pVDZ level of theory (percentage deviations from the monomer values are shown in parenthesis).

		–COO^-				–NH_3^+			
		monomer		dimer		monomer		dimer	
dimer	d(N···O)[a]	α_{ISO}	$\Delta\alpha$	α_{ISO}	$\Delta\alpha$	α_{ISO}	$\Delta\alpha$	α_{ISO}	$\Delta\alpha$
gly–gly-1	2.802			26.60(8%)	14.45(7%)			11.62(5%)	5.18(-24%)
gly–gly-2	2.970	24.56	13.47	26.54(8%)	19.10(42%)	11.06	6.89	11.97(8%)	7.68(11%)
gly–gly-3	2.807			25.66(4%)	17.44(29%)			11.56(5%)	5.83(-15%)
ala–ala-1	2.828	23.79	13.32	24.02(1%)	16.63(25%)	10.63	6.93	10.99(3%)	5.18(-25%)
ala–ala-2	2.849			24.31(2%)	16.12(21%)			11.73(10%)	7.63(10%)
leu–leu	2.678	23.33	12.90	22.63(-3%)	14.80(15%)	10.22	7.17	9.48(-7%)	6.04(-16%)
thr–thr	2.917	23.12	12.15	23.61(2%)	17.16(41%)	10.67	7.16	11.47(7%)	6.83(5%)
glu–glu	2.785	23.84	14.29	22.98(-4%)	13.58(-5%)	10.60	7.08	11.15(5%)	5.77(-19%)
cys–cys	2.780	23.93	13.83	23.65(-1%)	15.25(-11%)	7.57	5.65	7.83(3%)	5.33(-6%)
his–his	2.769	24.25	14.44	23.82(-2%)	15.58(8%)	10.89	5.04	11.76(8%)	6.68(20%)

[a] d(N···O) denotes the distance in Å between the hydrogen bond donor N atom of the –NH_3^+ group and the hydrogen bond acceptor O atom of the –COO^- group.

Table 7. Components of the dipole moment (*au*) for the glycine monomer and for the hydrogen-bonded acceptor and donor molecules in the gly-gly-1 dimer, along with the predictions calculated using RLFT. Computations are at the CAM-B3LYP/d-aug-cc-pVDZ level of theory.

Monomer					
		μ_x	μ_y	μ_z	$\|\boldsymbol{\mu}\|$
QTAIM	total	-1.39	0.15	4.47	4.69
	COO^-	0.36	-0.23	2.53	2.57
	NH_3^+	-1.19	0.34	0.49	1.33
	CH_2	-0.56	0.04	1.46	1.57

Dimer		Donor				Acceptor			
		μ_x	μ_y	μ_z	$\|\boldsymbol{\mu}\|$	μ_x	μ_y	μ_z	$\|\boldsymbol{\mu}\|$
QTAIM	total	-1.34	0.15	5.20	5.37	-1.25	0.12	4.96	5.11
	COO^-	0.36	-0.24	2.73	2.76	0.53	-0.26	2.85	2.91
	NH_3^+	-1.14	0.32	0.81	1.43	-1.24	0.35	0.55	1.40
	CH_2	-0.55	0.08	1.66	1.75	-0.53	0.03	1.56	1.65
RLFT3	total	-1.29	0.15	5.39	5.55	-1.20	0.12	5.01	5.15
	COO^-	0.35	-0.23	2.71	2.74	0.54	-0.25	2.96	3.02
	NH_3^+	-1.06	0.33	0.87	1.44	-1.20	0.34	0.54	1.36
	CH_2	-0.58	0.06	1.81	1.90	-0.54	0.03	1.52	1.61
RLFT1	total	-1.36	0.14	4.94	5.13	-1.36	0.14	4.94	5.13

Table 8. Static dipole polarizabilities (*au*) for the glycine monomer and for the hydrogen-bonded donor and acceptor molecules in the gly-gly-1 dimer, along with the predictions calculated using RLFT. Computations are at the CAM-B3LYP/d-aug-cc-pVDZ level of theory.

Monomer						
		α_{11}	α_{22}	α_{33}	α_{iso}	$\Delta\alpha$
QTAIM	total	35.78	49.31	57.88	47.66	19.30
	COO^-	15.71	27.69	30.32	24.57	13.49
	NH_3^+	8.42	9.19	15.62	11.08	6.85
	CH_2	10.16	11.05	13.72	11.64	3.21

Dimer		Donor					Acceptor				
		α_{11}	α_{22}	α_{33}	α_{iso}	$\Delta\alpha$	α_{11}	α_{22}	α_{33}	α_{iso}	$\Delta\alpha$
QTAIM	total	34.86	45.42	59.36	46.55	21.28	32.15	46.69	59.29	46.04	23.52
	COO^-	17.10	25.91	32.22	25.09	13.14	14.72	28.00	32.32	25.01	15.89
	NH_3^+	8.45	9.55	14.15	10.72	5.24	7.95	8.55	14.13	10.21	5.90
	CH_2	9.30	9.96	12.99	10.75	3.41	9.48	10.14	12.84	10.82	3.08
RLFT3	total	33.41	48.62	64.71	48.91	27.13	33.41	48.36	64.18	48.65	26.65
	COO^-	15.40	28.05	31.04	24.83	14.38	14.36	26.54	36.24	25.71	19.01
	NH_3^+	8.33	10.19	16.52	11.68	7.43	8.44	9.01	16.05	11.16	7.39
	CH_2	9.48	10.01	17.71	12.40	7.97	9.91	10.67	14.69	11.75	4.52
RLFT1		34.12	48.37	61.72	48.07	23.89	34.12	48.37	61.72	48.07	23.89

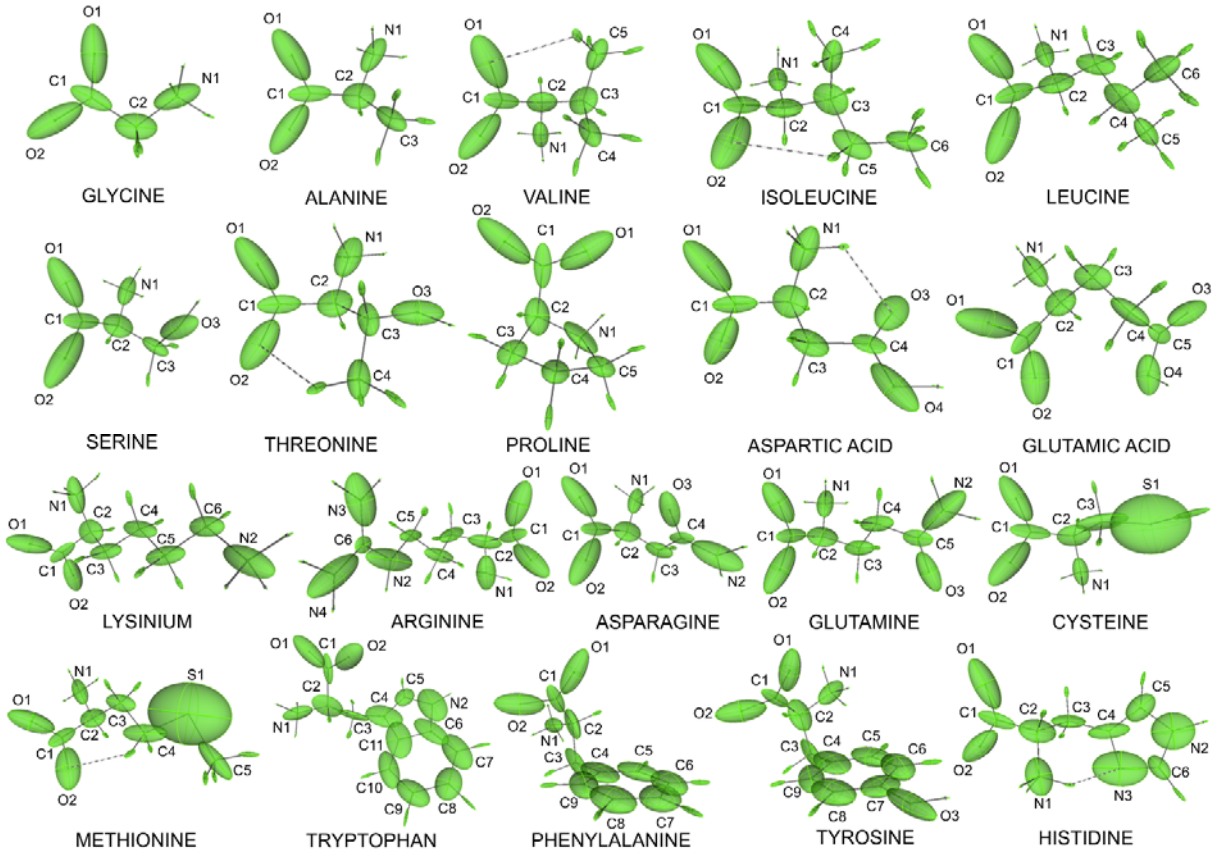

Figure 1. Atomic polarizability ellipsoids for the amino acids at the CAM-B3LYP/d-aug-cc-pVDZ level of theory. Intramolecular hydrogen bonds are shown as dashed lines.

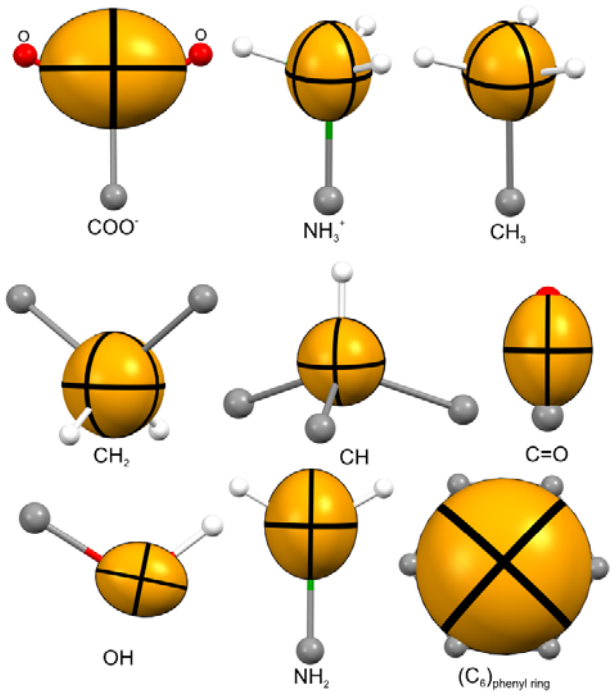

Figure 2. Polarizability ellipsoids for the main functional groups present in the amino acids at the CAM-B3LYP/d-aug-cc-pVDZ level of theory. Ellipsoids are centered at the center of mass of the functional groups.

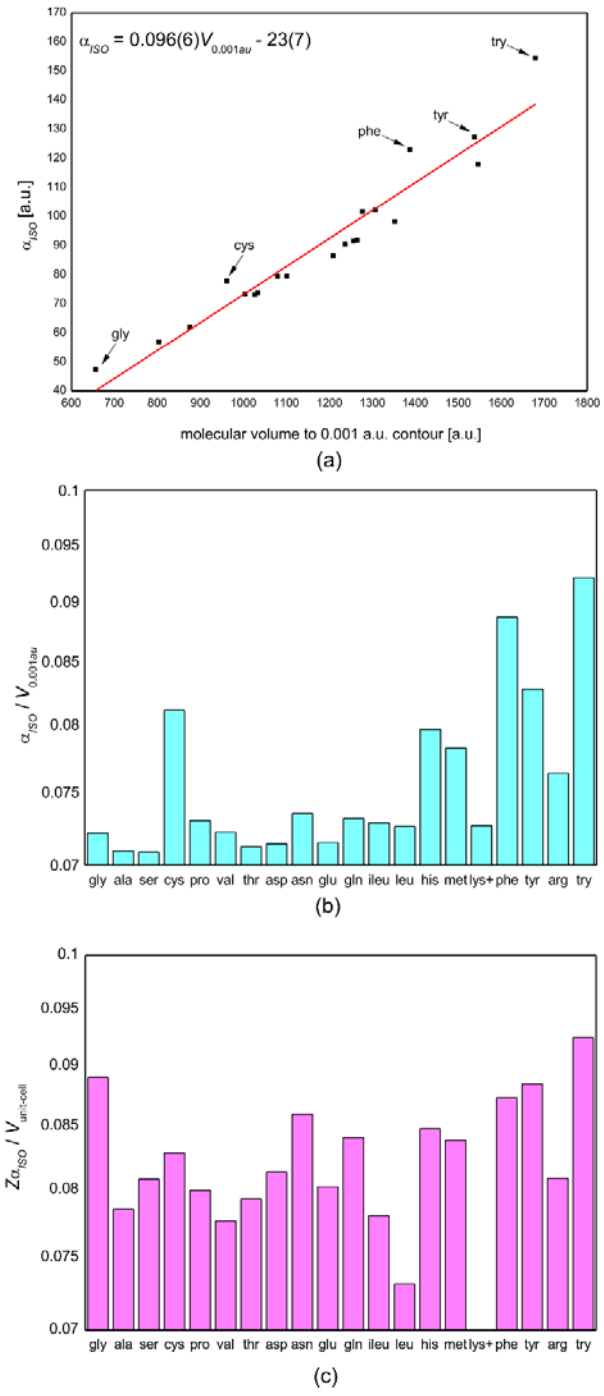

Figure 3. (a) Isotropic molecular polarizabilities plotted against the molecular volumes determined by a 0.001 *au* isosurface of electron density. (b) and (c) Polarizability densities for the amino acids. In (b), the molecular volume is defined by a 0.001 *au* isosurface of electron

density, while in (c) it is defined by the room-temperature unit cell volume. Z is the number of molecules per unit cell. All calculations were performed at the CAM-B3LYP/d-aug-cc-pVDZ level of theory.

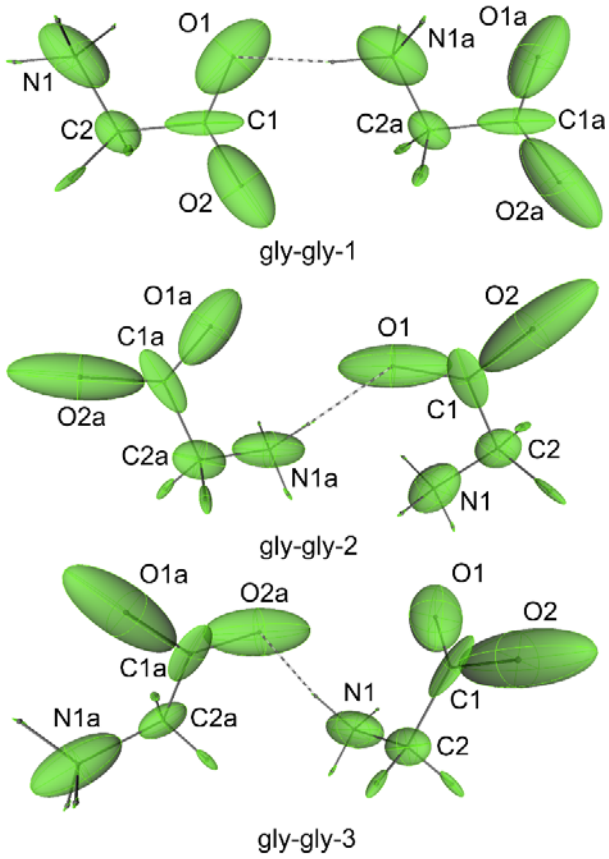

Figure 4. Atomic polarizability ellipsoids for three glycine dimers at CAM-B3LYP/d-aug-cc-pVDZ level of theory. Hydrogen bonds are shown as dashed lines. The N···O distance is 2.97 Å in gly-gly-2 and 2.80 Å in gly-gly-1 and gly-gly-3.

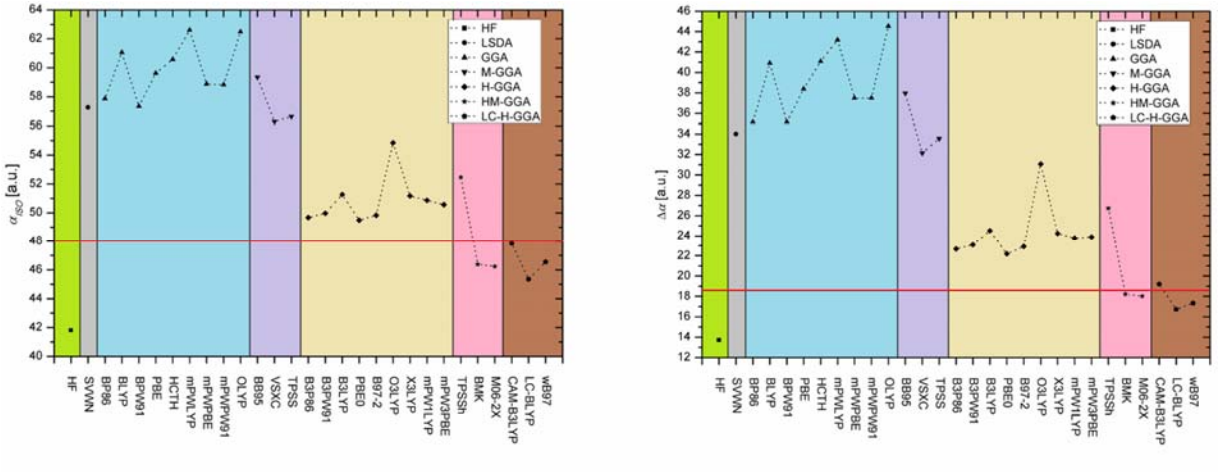

Figure 5. Isotropic polarizability and polarizability anisotropy of glycine calculated using various DFT functionals and comparison with the MP2 result (red line). All calculations employ the d-aug-cc-pVTZ basis set.

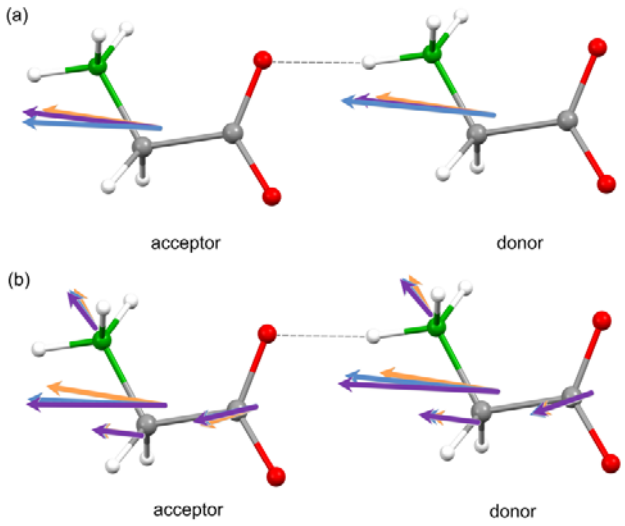

Figure 6. Dipole moments for the molecules in the gly-gly-1 dimer. Orange arrow: for the monomer; Blue arrow: calculated using QTAIM partition; Violet arrow: calculated using the RLFT models. (a) RLFT1 and (b) RLFT3.

FOR TABLE OF CONTENTS USE ONLY

Distributed Atomic Polarizabilities of Amino Acids and their Hydrogen-Bonded Aggregates

Leonardo H. R. Dos Santos,[*,†] *Anna Krawczuk,*[‡] *and Piero Macchi*[*,†]